Liquid Crystals
Publication details, including instructions for authors and subscription information:
http://www.informaworld.com/smpp/title~content=t713926090

Temperature behaviour of a liquid crystal comb polymer: Light scattering and noise of the scattered light

P. Allia[a]; C. Oldano[a]; M. Rajteri[a]; P. Taverna[a]; L. Trossi[a]; B. Gallot[b]; F. Monnet[b]
[a] Dipartimento di Fisica del Politecnico di Torino, and INFM, Torino, Italy [b] Laboratoire des Matériaux Organiques à Propriétés Specifiques, Vernaison, France

To cite this Article Allia, P. , Oldano, C. , Rajteri, M. , Taverna, P. , Trossi, L. , Gallot, B. and Monnet, F.(1996) 'Temperature behaviour of a liquid crystal comb polymer: Light scattering and noise of the scattered light', Liquid Crystals, 20: 2, 225 — 234
To link to this Article: DOI: 10.1080/02678299608031129
URL: http://dx.doi.org/10.1080/02678299608031129

LIQUID CRYSTALS, 1996, VOL. 20, NO. 2, 225–234

Temperature behaviour of a liquid crystal comb polymer: Light scattering and noise of the scattered light

by P. ALLIA*, C. OLDANO, M. RAJTERI, P. TAVERNA, L. TROSSI
Dipartimento di Fisica del Politecnico di Torino, and INFM, I-10129 Torino, Italy

B. GALLOT and F. MONNET
Laboratoire des Matériaux Organiques à Proprietés Specifiques, CNRS, F-69390 Vernaison, France

(*Received 6 April 1995; accepted 18 September 1995*)

Measurements of the intensity of the monochromatic light transmitted through and scattered by a comb polymer with a polyacrylamide main chain were performed between room temperature and the isotropization temperature of the polymer. The stationary noise of the light scattered at low angle was measured in the same temperature interval. The transmitted intensity is observed to increase strongly above the smectic S_{I_2}–S_{C_2} transition, where the intensity of the light scattered at low angles is maximized. The power dissipated by the molecular fluctuations dramatically increases above the transition between the two smectic phases. The spectral density curves display a Lorentzian character only below the S_{I_2}–S_{C_2} transition. At higher temperatures, a more complex frequency behaviour of the stationary noise spectra is observed. Such a behaviour is interpreted in terms of a model explicitly invoking the effect of the Brownian movement of segments of the main chain (backbone) of the polymer on the side chain fluctuations. The parameters governing the Brownian movements of both main and side chains, and their evolution with temperature, are determined and discussed in the light of a simple structural model.

1. Introduction

Increasing interest has recently been addressed to the physical and chemical properties of polymeric liquid crystals, owing to their intrinsic significance from the fundamentalist's viewpoint, and to their widespread prospective applications as elements of electro-optical devices.

Thermotropic side chain liquid crystal polymers (LCPs) are formed by a rigid mesogenic unit linked through a flexible spacer to a polymer backbone. These polymers combine typical macromolecular properties, such as easy processability and the possibility of freezing into the glassy state an orientation obtained at a higher temperature, with the typical properties of liquid crystals of low molecular weight, such as a variety of mesophase structures and the ability to give electro-optic response. As a consequence, LCPs are good candidates for applications in the field of electro-optical devices, such as displays, sensors, or modulators for optical-signal treatments [1,2].

Rather surprisingly, although the amide bond is much more stable than the ester linkage, polyacrylamide polymers have received limited attention, with the exception of some studies by Russian researchers, asserting that polymers with polymethacrylamide main chains and biphenyl mesogenic cores exhibit only crystalline structures [3], and of a series of papers on the synthesis and the X-ray diffraction study of polymers with polyacrylamide or polymethacrylamide main chains and lipopeptidic or liposaccharic side chains, showing that they display both thermotropic and lyotropic properties [4–9].

In a recent paper, some of the present authors (B.G. and F.M.) showed that comb polymers with a polyacrylamide main chain and undecanoylbiphenyl side chains exhibit two tilted bilayer smectic phases: an ordered S_{I_2} and a disordered S_{C_2} smectic phase, depending on the considered temperature range [10]. These polymers correspond to the chemical formula:

$$\begin{array}{l}(CH_2\text{–}CH)_n \\ \qquad | \\ \qquad CO\text{–}NH\text{–}(CH_2)_{10}\text{–}CO\text{–}C_6H_4\text{–}C_6H_5.\end{array}$$

Optical techniques have been traditionally exploited to study different aspects of the physics of liquid crystals [11]. In particular, the analysis of the intensity of the

*Author for correspondence.

light transmitted through, or scattered by these optically anisotropic media has been successfully introduced to investigate the details of the ordered liquid crystalline state [11]. The stationary noise of the light scattered by a liquid crystal is intrinsically interesting, being closely related to the equilibrium fluctuations of the component molecules, whose relaxation times are proportional to particular ratios of the viscous-to-elastic constants [11–13].

In the present paper, optical techniques have been variously exploited in order to investigate the possibility of applications of these polyacrylamide polymers in electro-optical devices. In particular, the parameters governing the Brownian movements of the polymeric main chains and of the side chains bearing the mesogenic biphenyl groups were studied for the first time by measuring the intensity of the light scattered by the material, and the associated stationary noise. The temperature evolution of these parameters and the effect of the transition between the two smectic phases were analysed for the polyacrylamide under consideration by studying the changes in the intensity of both scattered and transmitted light, and the evolution in the spectral density of the scattered-light noise between room temperature and the isotropization temperature.

2. Experimental

2.1. *Synthesis of the comb polymer and sample preparation*

Liquid crystalline comb polymers with a polyacrylamide main chain and polymethylene spacers derived fom the undecanoylbiphenyl mesogenic, side groups corresponding to the formula shown above, were prepared under an inert argon atmosphere by radical polymerization of acrylamidoundecanoylbiphenyl, at $T = 338$ K (65°C) in THF solution, with AIBN as initiator, as described elsewhere [10]. The molecular characteristics of the polymers ($M_n = 24460$, $M_w = 42350$ and $M_w/M_n = 1{\cdot}73$) were determined by light scattering using THF as solvent and Gel Permeation Chromatography using the same solvent [10].

The sample used for optical measurements was contained in a typical slab-type cell consisting of two parallel glass plates with a constant spacing of 50 μm ensured by mylar spacers. A thermoresistant glue was used to assemble the cell. The sample homogeneity was checked by polarized light microscopy.

2.2. *Structure of the comb polymer*

The structural features of these comb polymers were recently determined at different temperatures by means of X-ray diffraction. The details are given elsewhere [10], and only a brief account of the main points follows. An ordered, double-layer smectic structure (of S_{I_2} type) is observed below $T = 378$ K (105°C). It is characterized by a hexagonal arrangement of the side chains, evidenced by a narrow reflection of X-rays at wide angles, characteristic of such a type of packing [10]. The side chains are tilted of an angle $\theta = 18{\cdot}8°$ with respect to the normal to the smectic planes. These planes are defined by the main chains, which display a significant degree of parallel alignment in this phase. The distance between smectic planes turns out to be $d = 53$ Å. The disordered double-layer smectic structure (of S_{C_2} type) appears above $T = 378$ K, and is characterized by the same values of d and θ as for the ordered phase. The main chains still lie in the smectic planes, but their parallel alignment is lost. The isotropization temperature, as determined by X-ray diffraction, occurs at $T = 423$ K (150°C). In fact, this is the temperature at which the isotropization process is completed.

2.3. *Experimental set-up and procedure*

The experimental set-up for the light-scattering measurements is shown in figure 1 [14]. The light emitted by a 10 mW He–Ne laser (L) was filtered and focused on the sample through the pinhole PH and the converging lens L. The state of polarization of the light was determined by the polarizer P, and the intensity was controlled through a suitable neutral density filter ND. The sample LC was placed inside a small oven, electrically heated and connected to a temperature controller TC, ensuring a stability of ±1 K during the measurements. The light emerging from the sample and from the analyser A was detected by the photodiode PD, whose signal was amplified and sent either to the FFT signal analyser SA, providing the average power spectrum of the noise in the frequency range $2{\cdot}5 \times 10^{-2} < \nu < 2 \times 10^4$ Hz, or to the digital oscilloscope

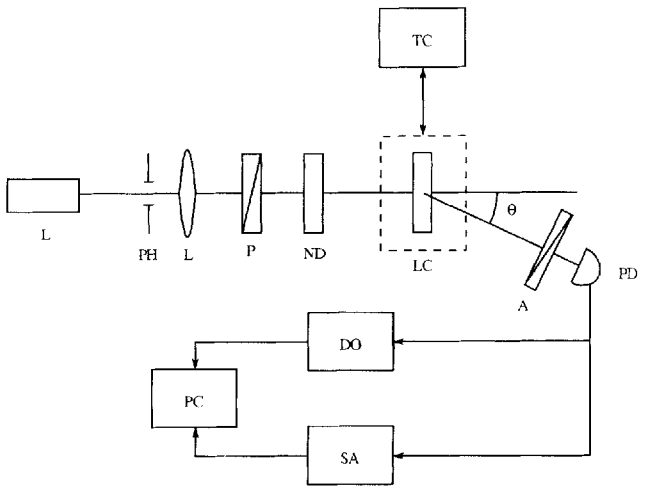

Figure 1. Experimental set-up for optical measurements; acronyms are defined in the text.

DO, exploited in the light intensity measurements. Both instruments were controlled by the computer PC. The photodiode was mounted on a platform, rotating in the incident plane around a vertical axis coincident with the sample, in order to explore different angles of scattering. All measurements were performed at normal incidence.

3. Results

3.1. *Transmitted and scattered light*

The temperature behaviour of the intensity of the light transmitted through the sample under normal incidence is shown in figure 2. In this case, the average heating rate (including measurement time) was about $1\,K\,min^{-1}$ below 353 K (80°C) and above 373 K (100°C), and was reduced to $0{\cdot}4\,K\,min^{-1}$ within this temperature interval. Below 353 K, the transmitted light intensity stays almost constant and low, indicating that most of the incident light is scattered at large angles by the sample. A sudden change in the slope of the curve occurs at 363 K. Above this temperature, the intensity steadily grows up to values 8 times larger than those observed at low temperature, displaying a tendency towards saturation in the high T limit, i.e. when the isotropic phase is approached.

The intensity of the light scattered by the sample at low and intermediate angles (scattering angle $\theta_s = 4°$, 6°, 10° in air) is reported in figure 3. In all cases, the heating procedure was the same as for the transmitted light measurements. At small angles (curves (*a*) and (*b*)), the intensity of the light scattered by the sample at low temperature is rather weak. Deviations from a linear behaviour in this temperature region merely reflect the experimental uncertainty. Above 355 K, the measured intensity suddenly increases, and both curves display a

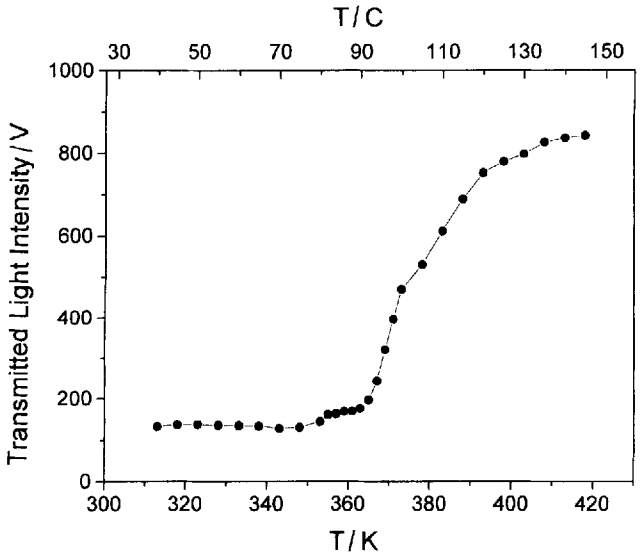

Figure 2. Temperature behaviour of the light transmitted through the polymer (angle of incidence $\theta_i = 0°$).

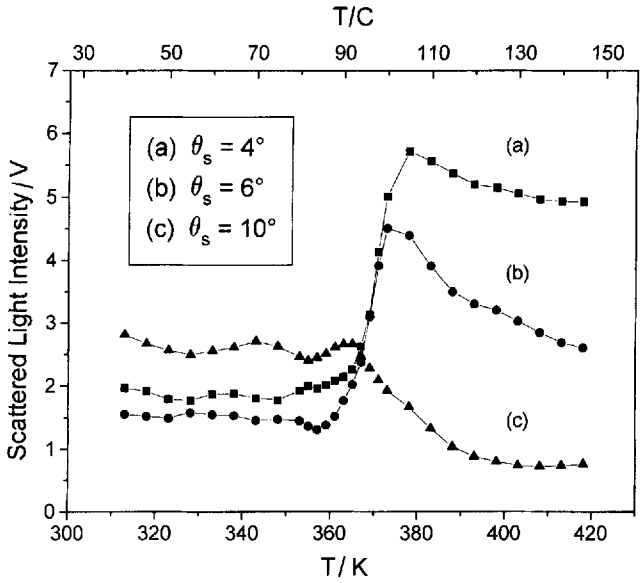

Figure 3. Temperature behaviour of the light scattered by the sample at three different angles θ_s (in air). Angle of incidence $\theta_i = 0°$.

maximum at about 375 K. Above this temperature, the scattered light intensity decreases on approaching the isotropic phase, as indeed is expected. It should be explicitly noted that the curve (*b*), measured at $\theta_s = 6°$, is more representative of the actual sample's behaviour than curve (*a*). The maximum of the latter curve appears to be broader than expected, and slightly displaced towards higher temperatures, owing to a double reflection of the direct beam. At low scattering angles, in fact, a small fraction of the transmitted beam was partially reflected by the outer ring of the photodiode holder back to the sample holder, which acted as a secondary source of diffuse light. Although this effect was minimized by using a small reflector to prevent most of the direct beam from impinging on the photodiode holder, the intensity ratio between transmitted and scattered light was so high (see the y axis scales in figures 2 and 3) that curve (*a*) was still affected, to some extent, by the direct beam, whose intensity increased with T, giving rise to a slower decrease in the high temperature scattered intensity. For scattering angles larger than 5°, the direct beam was no longer reflected by the photodiode holder.

Curve (*c*) displays a completely different behaviour. Although at low temperatures the intensity of the light scattered from the sample region examined is almost constant and higher than in cases (*a*) and (*b*), the observed signal begins to decrease at $T \cong 363$ K, without showing any defined maximum, and finally reaches a very low saturation value in the high T limit.

Isothermal measurements of the scattered light were

performed as functions of the scattering angle θ_s in the interval $0 \leqslant \theta_s \leqslant 20°$ in air. Higher scattering angles were not experimentally accessible owing to the sample holder's shadow. Measurements at very low θ_s were performed by suitably attenuating the light of the incident beam, to avoid saturation of the amplified photodiode. The results for $T = 313$ K (40°C) and $T = 403$ K (130°C) are reported in figure 4. Both curves monotonically decrease with θ_s, as expected. However, above $\theta_s \cong 5°$ the slope of the curve is strongly reduced, giving rise to an extended tail. This result indicates that a large fraction of the light incident on the material under study is actually scattered at large angles. Generally speaking, other anisotropic media, like nematic liquid crystals (either bulk or polymer-dispersed) are characterized by a much narrower peak of the scattered intensity around $\theta_s = 0$, with no such tails at high scattering angles [14].

As observed in figure 4, the intensity of both transmitted ($\theta_s = 0°$) and scattered light is lower at $T = 313$ K than at $T = 403$ K, at least up to $\theta_s \cong 8°$, where the curves cross. This behaviour is in good agreement with the data reported in figures 2 and 3. Note that the data reported in figure 4 refer to an average over curves taken on different sample regions. Although the curves corresponding to any single region display the same trend with θ_S, they are affected to a larger extent by irregular fluctuations in the signal picked-up as a function of θ_B, presumably attributable to the zones of coherence of the laser light.

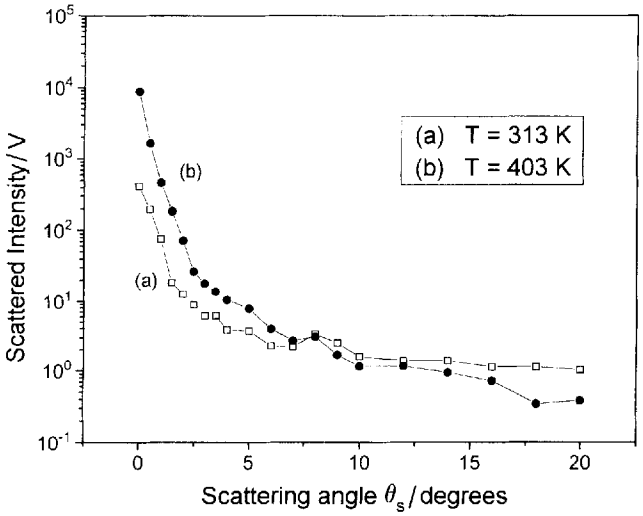

Figure 4. Representative behaviour of the intensity of the light scattered by the sample as a function of the scattering angle, in the S_{I_2} and S_{C_2} phases of the polymer (curves (*a*) and (*b*), respectively) of the polymer. The data correspond to an average over measurements performed on many different sample regions.

It should be remarked that the intensity of the light scattered by the sample at low angles peaks at a temperature corresponding, within the experimental uncertainty, to the S_{I_2}–S_{C_2} transition of the comb polymer.

3.2. *Stationary noise of the scattered light*

The stationary noise of the light scattered by the sample at a low angle ($\theta_s = 4°$ in air) was measured as a function of temperature from 313 K (40°C) to 428 K (155°C). The measurements were performed at the same average rates of heating and cooling (0·5 K min^{-1}, including measurement time). Three representative power spectra of the scattered light noise are reported in figure 5. All curves were obtained in the frequency range $0{\cdot}05\ \text{Hz} \leqslant \nu \leqslant 20\ \text{Hz}$. For higher frequencies, all curves merge in the background noise, independently of the temperature. The background noise increases by less than one order of magnitude in the considered temperature range. The low T spectra appear to be well described by a single Lorentzian function. However, the Lorentzian character disappears with increasing T above about 370 K, and the curves obtained at the highest temperatures (for example, curve (*c*) in figure 5) show a much steeper high frequency decay than expected with a Lorentzian function.

The power-density curves were integrated in order to get information about the role of temperature on the molecular fluctuations. As a matter of fact, the value obtained by integrating the whole power spectrum of a stationary noise is proportional to the total power dissipated by the microscopic fluctuation processes

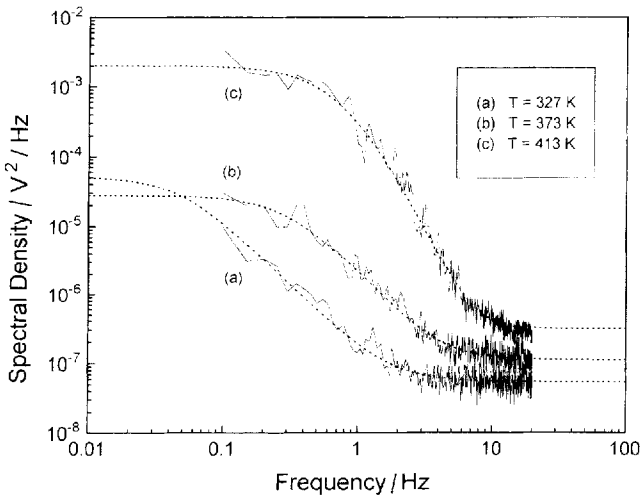

Figure 5. Representative power spectra of the stationary noise of the light scattered by the sample at three different temperatures. Scattering angle $\theta_s = 4°$ (in air). Dotted lines: Lorentzian function, $S_1(\nu)$ (curve (*a*)); $S_2(\nu)$ function (curves (*b*) and (*c*)).

responsible for the noise [15]. In this case, the small background noise was subtracted before integrating, and the contributions from very low frequencies, not experimentally accessible, may be easily shown to be almost negligible in determining the integrated power of the signal. The results of the integration are shown in figure 6 for both heating and cooling (full and open circles, respectively). On heating, the integrated power stays constant up to about 370 K, and grows monotonically in the interval $370\,K \leqslant T \leqslant 420\,K$ (note the logarithmic scale). At higher temperatures, the integrated power seems to jump to very large values. However, too few data were obtained in this temperature range to allow definite conclusions to be reached about this effect. It should be noted that at $T \geqslant 430\,K$, polymer contamination by liquefying of the glue used to bind the sample cell becomes possible after a certain time. On cooling, the integrated power follows a similar curve displaced towards lower temperatures, showing a hysteric behaviour. The area defined by the spectral-density curve becomes vanishingly small at about 360 K. The temperature difference between points corresponding to the same level of integrated power on the heating and cooling curves increases with T. The effect is reversible, i.e. if the sample is reheated after a first heating–cooling cycle, the integrated power follows again the curve defined by the full circles in figure 6.

4. Analysis of the spectral-density curves

The evolving character of the measured spectra from a pure Lorentzian to a non-Lorentzian curve may be expressed in terms of a simple functional law. First, let us briefly discuss the possible sources of the scattered light noise. At temperatures much lower than 370 K, the polymer main chains are frozen in the smectic planes, and rigidly aligned, so that the corresponding side chains are arranged at the vertexes of regular hexagons [10]. As a consequence, the measured noise must arise from the fluctuation of side chains. It is reasonable to assume that the optical noise observed in the explored frequency range arises at all temperatures from the Brownian movement of side chains.

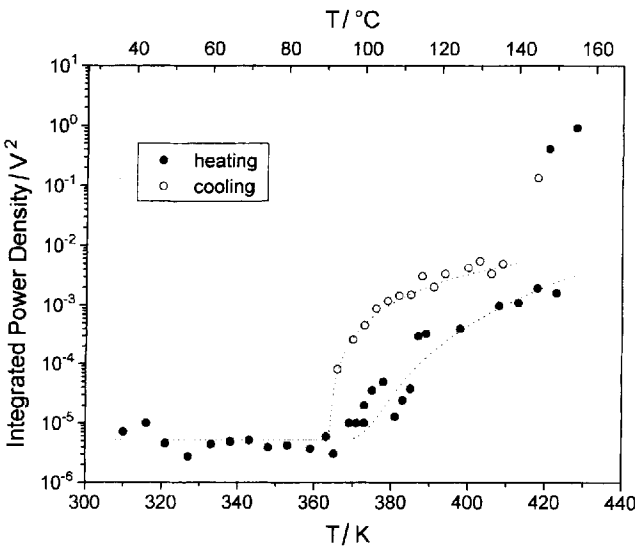

Figure 6. Hysteretic temperature behaviour of the area of the measured power spectra of the scattered light. Full circles: heating; open circles: cooling.

Low temperature spectra are well fitted to an expression of the type

$$S_1(\nu) = S_0(T) + \frac{P_1}{\nu^2 + \gamma_1^2} \tag{1}$$

where $S_0(T)$ is a white spectrum representing the background, P_1 is an amplitude, and γ_1 is a cut-off frequency. The dotted line superimposed to curve (*a*) of figure 5 is an example of the results of such a fitting procedure. It should be noted that low T spectra appear as non-saturating in their low frequency side (see curve (*a*) of figure 5) because their cut-off frequency is definitely below the lower limit of the chosen frequency window. In these cases, the cut-off frequency is obtained by admitting that the experimental data represent the high frequency tail of a Lorentzian function.

Higher temperature spectra are instead described by a more complex frequency law, of the type

$$S_2(\nu) = S_0(T) + \left(P_1 + \frac{P_2}{\nu^2 + \gamma_2^2}\right)\frac{1}{\nu^2 + \gamma_1^2} \tag{2}$$

where S_0 is a white spectrum, P_1 and P_2 are temperature-dependent weighting factors (with different physical dimensions) and γ_1, γ_2 are cut-off frequencies. The S_2 function is the weighted sum of a pure Lorentzian and the product of two Lorentzians. Obviously, S_2 reduces to S_1 when $P_2 = 0$. An example of the agreement between equation (2) and the experimental curves is given by the dotted lines superimposed to curves (*b*) and (*c*) in figure 5. All high T spectra are accurately described by the $S_2(\nu)$ function.

The temperature behaviour of the cut-off frequencies γ_1 and γ_2 resulting from the analysis of spectra measured during sample heating is shown in figure 7, while the behaviour of P_1 and P_2 is reported in figure 8. It should be noted that, while $P_1(T)$ is different from zero over the whole explored temperature range, and increases smoothly with T, $P_2(T)$ remains equal to zero up to about 365 K, and subsequently grows with temperature, first weakly between 365 and about 385 K (the effect is barely visible on the scale of figure 8 (*b*)), then strongly, according to a nearly linear law. Similarly, the cutoff frequency γ_1 is a smooth function of T, increasing from

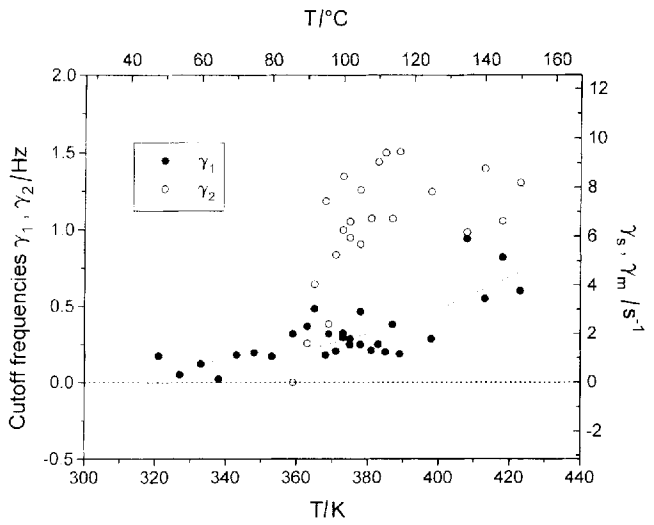

Figure 7. Temperature behaviour of the cut-off frequencies γ_1 and γ_2 appearing in the $S_2(\nu)$ fitting function (see text).

about 0·2 Hz at 320 K to about 0·75 Hz at 420 K. On the contrary, γ_2 (which is obviously defined only when $P_2 \neq 0$) rapidly increases from zero to about 1·1 Hz when the temperature is changed from 360 K to 370 K. At higher temperatures, γ_2 is observed to increase at a much more reduced rate.

Although the considered best-fit parameters are all rather scattered, the evidence for a complex functional dependence of the observed spectra on both frequency and temperature is unequivocal.

5. A simple model of optical noise in comb polymers

The stationary noise of the light scattered from optically anisotropic media, such as liquid crystals, is related to the Brownian movement of the molecules of the materials which are submitted to a stochastic thermal force, representing the effect of random collisions. Usually, the collision force in thermal equilibrium is assumed to have a white spectrum. In the present case, however, the noise observed in the considered frequency interval is supposed to originate from fluctuations of the polymer side chains, as discussed before. According to the current views about structure and structural changes in comb polymers, it is reasonable to assume that the total stochastic force per unit mass acting on the polymer side chains, f_s, may be expressed as the sum of two terms, having different spectral contents:

$$f_s = f + f_m \tag{3}$$

where f is the usual collision force and f_m is an extra force representing the effect of random movements of the main chain on the side chains, according to the picture of figure 9. This assumption is justified, recognizing that the main chains are progressively losing order

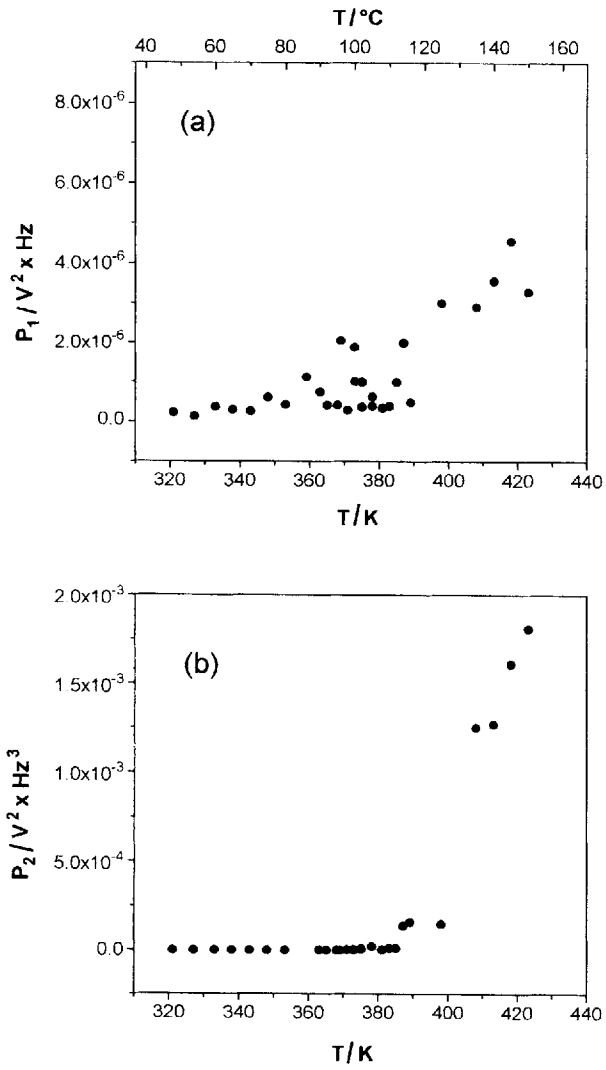

Figure 8. Temperature behaviour of the weighting factors of Lorentzian (P_1) and non-Lorentzian (P_2) components of the $S_2(\nu)$ fitting function.

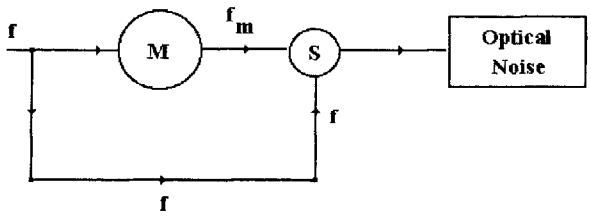

Figure 9. Picture of the model for optical-noise generation in a comb polymer. M: main chains; S: side chains; f: stochastic collision force; f_m: stochastic force exerted on side chains by the moving main chains.

and rigidity above about 360 K. Segments of these chains may then experience thermally-induced generalized displacements (bending, twisting), thereby exerting additional forces on the corresponding side chains.

As usual [15], the thermal force f is assumed to be characterized by a delta-like autocorrelation function $R_f(\tau)$, corresponding to a white power spectrum $S_{ff}(\omega)$:

$$\left.\begin{aligned} R_f(\tau) &= \lim_{T\to\infty}\frac{1}{2T}\int_{-T}^{T} f^*(t)f(t+\tau)\mathrm{d}t = \alpha\delta(\tau) \\ \text{and} \\ S_{ff}(\omega) &= \frac{1}{(2\pi)^{1/2}}\int_{-\infty}^{\infty} R_f(\tau)\,\mathrm{e}^{-\mathrm{i}\omega\tau}\mathrm{d}\tau = \alpha \end{aligned}\right\} \quad (4)$$

where α is a constant.

The extra force f_m is supposed to be proportional to a generalized displacement y of a main chain (or a segment of it) from the equilibrium position:

$$f_m = \kappa y \quad (5)$$

where k is a constant having dimensions $[\text{time}]^{-2}$. In these systems, as in all liquid crystals [12], a molecule is assumed to be subjected not only to collision forces, but also to external forces of an elastic nature, proportional to its displacement, and to viscous forces, proportional to its velocity. Moreover, the inertia term is generally negligible, so that the random variable y satisfies a Langevin equation for an overdamped oscillatory system:

$$\beta_m\dot{y} + \omega_m^2 y = f \quad (6)$$

where all hindrances to molecular motion are simply represented by a single damping force with damping coefficient β_m, and where ω_m is the frequency of free oscillation of the main chains. Under these conditions, the power spectrum of the random displacement y is [15]

$$S_{yy}(\omega) = \frac{1}{\beta_m^2}\frac{\alpha}{\omega^2+\gamma_m^2} \quad (7)$$

where $\gamma_m = \omega_m^2/\beta_m$ is the cut-off frequency of the process. By using equation (5) and the general properties of power spectra [15], one also gets $S_{f_m f_m} = \kappa^2 S_{yy}$.

The power spectrum of the total stochastic force acting on side chains is [15]

$$S_{f_s f_s}(\omega) = S_{ff}(\omega) + S_{f_m f_m}(\omega) + S_{ff_m}(\omega) + S_{f_m f}(\omega). \quad (8)$$

The cross terms in equation (8) cannot be neglected in this case, because the stochastic forces f and f_m are not statistically independent. By taking into account the general expression of the cross-spectra of two stochastic variables related through equations (5) and (6), one gets [15]

$$S_{ff_m} + S_{f_m f} = 2\,\mathrm{Re}\,\{S_{ff_m}\} = 2\kappa\alpha\frac{\omega_m^2}{\beta_m^2}\frac{1}{\omega^2+\gamma_m^2} \quad (9)$$

so that

$$S_{f_s f_s} = \alpha + \frac{\alpha}{\beta_m^2}(\kappa^2 + 2\kappa\omega_m^2)\frac{1}{\omega^2+\gamma_m^2}. \quad (10)$$

On the other hand, the generalized stochastic displacement x of side chains submitted to the force f_s satisfies an equation similar to equation (6):

$$\beta_s\dot{x} + \omega_s^2 x = f_s \quad (11)$$

where the parameters β_s, ω_s refer now to side chains and have an obvious meaning. Once again, all hindrances to molecular motion are described by a single damping term.

By definition, the power spectrum of the stochastic variable x (which is proportional to the measured spectrum of the optical noise) is

$$S_{xx}(\omega) = \frac{1}{\beta_s^2}\frac{S_{f_s f_s}(\omega)}{\omega^2+\gamma_s^2} \quad (12)$$

where γ_s is the cut-off frequency of side chain fluctuations. Inserting equation (10) into equation (12), and adding a constant background term S_o, one gets

$$S_{xx}(\omega) = S_o + \frac{1}{\beta_s^2}\left[\alpha + \frac{\alpha}{\beta_m^2}(\kappa^2+2\kappa\omega)\frac{1}{\omega^2+\gamma_m^2}\right]\frac{1}{\omega^2+\gamma_s^2}. \quad (13)$$

$S_{xx} - S_o$ is therefore the sum of a pure Lorentzian function, $S_L(\omega)$, corresponding to the white component of the spectrum of f_s:

$$S_L(\omega) = \frac{\alpha}{\beta_s^2}\frac{1}{\omega^2+\gamma_s^2} \quad (14)$$

and of a non-Lorentzian component, $S_{NL}(\omega)$, corresponding to the Lorentzian component of the spectrum of f_s:

$$S_{NL}(\omega) = \frac{\alpha\mu^2}{\beta_s^2\beta_m^2}\frac{1}{(\omega^2+\gamma_m^2)(\omega^2+\gamma_s^2)} \quad (15)$$

where $\mu^2 = \kappa^2 + 2\kappa\omega_m^2$. The model's prediction is in full agreement with the experimental results. By comparing equations (14) and (15) to equations (1) and (2), the following correspondences are found:

$$\left.\begin{aligned} &\frac{P_1}{\nu^2+\gamma_1^2} \Leftrightarrow \frac{\alpha}{\beta_s^2}\frac{1}{\omega^2+\gamma_s^2} \\ \text{and} \\ &\frac{P_2}{(\nu^2+\gamma_2^2)(\nu^2+\gamma_1^2)} \Leftrightarrow \frac{\alpha\mu^2}{\beta_s^2\beta_m^2}\frac{1}{(\omega^2+\gamma_m^2)(\omega^2+\gamma_s^2)}. \end{aligned}\right\} \quad (16)$$

Therefore, $\gamma_s = 2\pi\gamma_1$ and $\gamma_m = 2\pi\gamma_2$. According to the theory [15], the white noise value α is given by

$$\alpha = 2kT\beta_s \quad (17)$$

where k is the Boltzmann's constant and β_s is the damping coefficient for the polymer side chains, responsible for the measured optical noise. By using equation (17) and the first relation (16), the following proportionality may be established:

$$P_1 \approx \frac{\alpha}{\beta_s^2} \approx \frac{T}{\beta_s} \tag{18}$$

so that

$$\beta_s(T) \approx \frac{T}{P_1(T)}. \tag{19}$$

It should be noted that the correct proportionality factor in equation (19) cannot be determined. Actually, the measurements considered do not directly provide the spectrum of the fluctuations of scattering molecules, S_{xx}, but the spectrum of the scattered light, S_2, which is proportional to S_{xx} through largely unknown experimental parameters. By using equation (17) and the second relation (16), one gets instead

$$\frac{P_1}{P_2} \approx \frac{\alpha}{\beta_s^2} \frac{\beta_s^2 \beta_m^2}{\alpha \mu^2} = \frac{\beta_m^2}{\mu^2}. \tag{20}$$

Admitting that μ^2 does not vary much with temperature, the following expression is obtained:

$$\beta_m(T) \approx \left[\frac{P_1(T)}{P_2(T)}\right]^{1/2}. \tag{21}$$

The quantities T/P_1 and $(P_1/P_2)^{1/2}$ deriving from the analysis of experimental data are reported in figures 10 and 11 as functions of temperature.

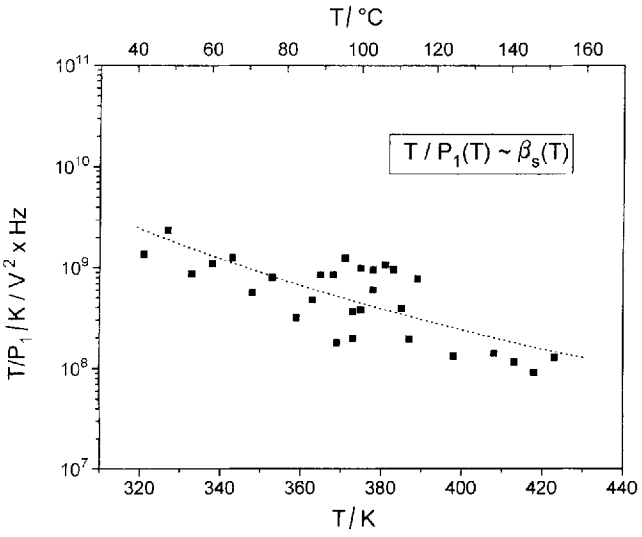

Figure 10. Behaviour of T/P_1 (proportional to the damping coefficient for polymer side chains) as a function of temperature. Dotted line: best fit to an Arrhenius law.

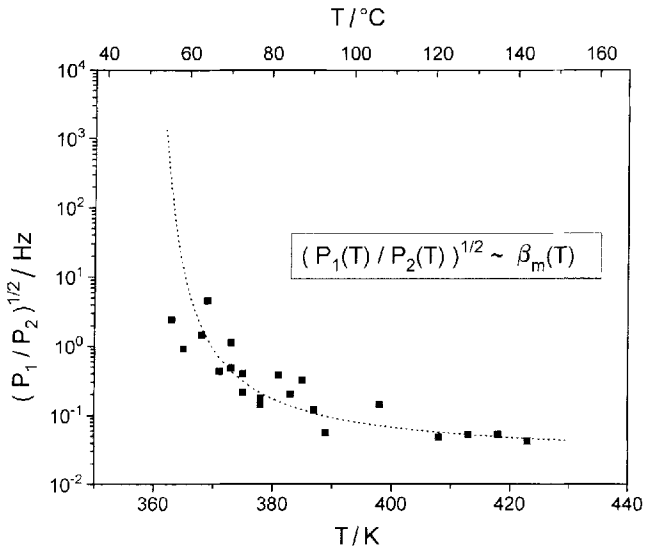

Figure 11. Behaviour of $(P_1/P_2)^{1/2}$ (approximately proportional to the damping coefficient for the polymer main chains) as a function of temperature. Dotted line: best fit to a Vogel–Fulcher–Taumann law.

The damping parameter β_s should involve an effective value of the viscosity experienced by the side chains. As a matter of fact, its temperature dependence turns out to be well described by an Arrhenius law:

$$\beta_s(T) = \beta_{so} \exp(Q/RT) \tag{22}$$

where β_{so} is a constant, Q is an activation energy for viscous flow, and R is Meyer's constant (dotted line in figure 10). A linear dependence of $\ln(T/P_1)$ on T^{-1} is actually found, providing the value $Q \cong 28{\cdot}5\,\mathrm{kJ\,mol^{-1}}$ (see figure 12(*a*)).

On the contrary, $\beta_m(T)$ is not defined below a given temperature T_o, and is observed to decrease very rapidly with increasing T above T_o, where this parameter appears to diverge. Such a behaviour is accurately described by a Vogel–Fulcher–Taumann expression:

$$\beta_y \approx \beta_{yo} \exp[\theta/(T - T_o)] \quad (T > T_o) \tag{23}$$

where β_{y0}, θ and T_o are constants (dotted line in figure 11). Writing $(P_1/P_2)^{1/2} = A \exp[B/(T - T_o)]$, and using the value for A derived from figure 11 in the high temperature limit, a linear relation is obtained when $[\ln(P_1/P_2)^{1/2} - \ln A]^{-1}$ is plotted versus T (see figure 12(*b*)), giving $T_o = 358\,\mathrm{K}$.

The present analysis provides therefore a complete picture of the evolving behaviour of both main chains and side chains of the considered comb polymer. The main chains are completely frozen at temperatures lower than T_o, which is 20 K below the temperature of the S_{I_2}–S_{C_2} transition, obtained through X-ray scattering (378 K) [10]. This means that the transition proper is

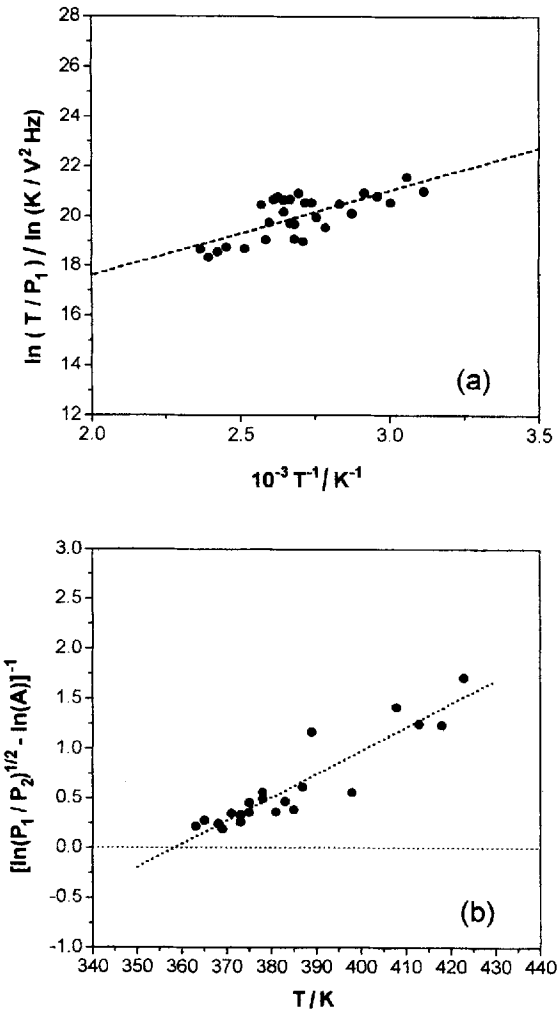

Figure 12. Plots used to determine the activation energy for the viscous flow of side chains (curve (*a*)) and the freezing temperature of main chains (curve (*b*)).

completed when the main chains have definitely lost their rigidity and can begin to perform collective, large scale movements, whilst remaining on the smectic planes. Moreover, at T_0 the characteristic relaxation time, $\tau_m = 1/\gamma_m$, is infinitely large. The random movements of the main chains are therefore vanishingly small and extremely slow when T is just above T_0. When the temperature is further increased, their amplitude grows and the relaxation time soon becomes of the order of 1 s. Actually, T_0 may correspond to the glass transition of the polymer main chain, not observable by DSC because the peak associated with the S_{I_2}–S_{C_2} transition covers the temperature domain 352–379 K (79–106°C), with a maximum found at 373 K (100°C). The side chain fluctuations are instead characterized by a relaxation time $\tau_s = 1/\gamma_s$ which remains finite over the whole explored temperature interval. It is noteworthy that no peculiar feature of the γ_s versus T curve is observed in the region where the main chain fluctuations freeze. This result points to a substantial statistical independence of these two types of fluctuations. The damping coefficient for side chains is found to follow an Arrhenius law similar to the one used to describe the isotropic viscosity of simple liquids [16]. The activation energy for viscous flow emerging from the present analysis, $Q = 28{\cdot}5\,\mathrm{kJ\,mol^{-1}}$, may be compared, for example, with the activation energies for the rotational viscosity in a number of liquid crystal systems, such as MBBA, HBAB, PAA (typically ranging between 40 and $50\,\mathrm{kJ\,mol^{-1}}$), and for the non-critical viscosity in the LC S_B phase of BBOA ($46{\cdot}1\,\mathrm{kJ\,mol^{-1}}$) [17].

6. Conclusions

The analysis of the properties of the light scattered by a comb polymer has proven useful to investigate, over an extended temperature interval, the evolution of both the structure of the material and of various parameters governing the Brownian movements of the component molecules.

The optical data have been given a more sound interpretation using the results of previous structural studies, allowing one to determine the different states of molecular order characterizing the component molecules in different temperature ranges. At low temperatures, in the S_{I_2} phase, the polymer acts as a strong scatterer of the incident light, so that a non-negligible fraction of the incident intensity is scattered at large angles. In the proximity of the S_{I_2}–S_{C_2} transition, as determined by X-ray diffraction, the intensity of the light transmitted by the sample begins to increase rapidly, and the light scattered at low angles displays a maximum, whose position corresponds to the abrupt change in slope of the transmitted intensity versus temperature curve. Both such features are therefore correlated with the partial disordering of polymer main chains, which lose their parallelism and give rise to a disordered smectic C phase for the side chains. Increasing the temperature, the intensity of the light scattered at low angles is somewhat reduced, indicating a tendency towards the isotropization of the optical properties. The smectic-to-isotropic transition proper occurs however at a temperature (423 K, as deduced by X-ray diffraction [10]) where accurate optical measurements were not permissible because of a possible contamination of the material from the glue used to bond the cell. The present results may indicate that a partial loss of the smectic order takes place gradually in the smectic phase with increasing temperature. It should be noted that the isotropization temperature of the material, as determined by polarized light microscopy (403 K) [10], is much lower than that indicated by X-ray diffraction, supporting the hypothesis

of a broad transformation, extending over a rather large temperature interval. This interval could result from the polydispersity of the polymer, the isotropization temperature being lower for molecules having a lower molecular weight than for the heavier molecules. In addition, it should be noted that X-ray diffraction generally gives higher transition temperatures than other methods, because it actually indicates the temperature at which all the molecules have performed the considered transition.

A considerable amount of information about the parameters governing the motion of both side chains and main chains may be extracted from the analysis of the noise of the light scattered at low angles by the polymer. In particular, two different temperature regions are identified. At all temperatures, the observed noise arises from side chain fluctuations. Below $T_0 = 358\,K$, the noise is characterized by a low intensity level and a Lorentzian frequency dependence. In the high temperature region, the noise level rapidly increases, and the frequency dependence becomes more complex. The experimental observations may be accounted for by admitting that the Brownian movements of side chains are affected not only by the usual, white noise fluctuation force, but also by the random motion of the main chains (or segments of them). In this way, it is possible to determine (i) the relaxation times of the fluctuations of both side chains and main chains and (ii) the effective damping coefficients for the motion of both types of chains. The latter parameters clearly involve two distinct effective viscosity constants for side chains and main chains. Below the freezing temperature $T_0 = 358\,K$ (possibly corresponding to the glass transition temperature of the main chains), 20 K below the S_{I_2}–S_{C_2} transition temperature as determined by X-ray diffraction, the main chains do not participate at all in the random movements giving rise to the noise of the scattered light. Above T_0, both a damping coefficient for the main chain movements, and a relaxation time may be defined. This result indicates that segments of the main chains begin to fluctuate incoherently in the S_{I_2} phase well before the completion of the structural transformation to the S_{C_2} phase, which requires the collective motion of main chains over large scale distances. The dynamic properties of side chains are little affected by structural changes: in fact, the relaxation times of their fluctuations, and the damping parameter describing the hindrances to their movements, are both regular over the whole considered temperature interval. The damping parameter follows an Arrhenius law, like some viscosity coefficients in other liquid crystal systems. The activation energy for viscous flow of the side chains is however smaller (by a factor of 0·7) than in other types of liquid crystal, indicating that the molecular movements responsible for the observed noise are comparatively easier in this comb polymer.

References

[1] McArdle, C. B., 1989, *Side chain Liquid Crystal Polymers*, edited by C. B. McArdle (Blackie), p. 1.

[2] Dubois, J. C., 1995, *Polym. Adv. Technol.*, **6**, 10.

[3] Shibaev, V. P., Plate', N. A., Smolianski, A. L., and Voloskov, A. K., 1989, *Makromolek. Chem.*, **181**, 1393.

[4] Gallot, B., and Douy, A., 1987, *Molec. Cryst. liq. Cryst.*, **153**, 367.

[5] Gallot, B., and Douy, A., 1989, *Makromolek. Chem., Macromolek. Symp.*, **24**, 321.

[6] Gallot, B., and Marchin, B., 1989, *Liq. Cryst.*, **5**, 1719.

[7] Gallot, B., and Diao, T., 1992, *Polymer*, **19**, 1719.

[8] Gallot, B., and Marchin, B., 1989, *Liq. Cryst.*, **5**, 1729.

[9] Gallot, B., Revilla, J., Charreyre, M. T., and Pichot, C., 1994, *Liquid Crystalline Polymers*, edited by C. Carfagna (London: Pergamon).

[10] Gallot, B., and Monnet, F., 1995, *Eur. Polym. J.* (in the press).

[11] De Gennes, P., 1975, *The Physics of Liquid Crystals* (Oxford: Clarendon Press), p. 59.

[12] Miraldi, E., Trossi, L., Taverna Valabrega, P., and Oldano, C., 1980, *Nuovo Cim. B*, **60**, 165.

[13] Allia, P., Galatola, P., Oldano, C., Taverna Valabrega, P., Trossi, L., and Aprato, C., 1993, *Molec. Cryst. liq. Cryst.*, **25**, 23.

[14] Allia, P., Oldano, C., Rajteri, M., Taverna, P., Trossi, L., and Aloe, R., 1994, *Liq. Cryst.*, **18**, 555.

[15] Papoulis, A., 1965, *Probability, Random Variables and Stochastic Processes* (New York: McGraw-Hill–Kogakusha), p. 336.

[16] Temperley, H. N. V., 1968, *Physics of Simple Liquids*, edited by H. N. V. Temperley, J. S. Rowlinson and G. S. Rushbrooke (Amsterdam: North Holland), p. 1.

[17] Tsykalo, A. L., 1991, *Thermophysical Properties of Liquid Crystals* (New York: Gordon and Breach), p. 100.